GYNECOLOGIC ONCOLOGY

Smooth muscle tumours of the uterus: MR imaging malignant predictive features—a 12-year analysis in a referral hospital in Portugal

Patrícia Freitas[1] · Teresa Resende-Neves[2] · Pedro Lameira[3] · Marta Costa[2] · Paulo Dias[4] · Juliana Filipe[5] · Joana Ferreira[5] · Ana Félix[5,6] · Teresa Margarida Cunha[4]

Abstract

Purpose To evaluate the magnetic resonance imaging (MRI) features that may help distinguish leiomyosarcomas from atypical leiomyomas (those presenting hyperintensity on T2-W images equal or superior to 50% compared to the myometrium).

Materials and methods The authors conducted a retrospective single-centre study that included a total of 57 women diagnosed with smooth muscle tumour of the uterus, who were evaluated with pelvic MRI, between January 2009 and March 2020. All cases had a histologically proven diagnosis (31 Atypical Leiomyomas—ALM; 26 Leiomyosarcomas—LMS). The MRI features evaluated in this study included: age at presentation, dimension, contours, intra-tumoral haemorrhagic areas, T2-WI heterogeneity, T2-WI dark areas, flow voids, cyst areas, necrosis, restriction on diffusion-weighted imaging (DWI), apparent diffusion coefficient (ADC) values, signal intensity and heterogeneity after contrast administration in T1-WI, presence and location of unenhanced areas. The association between the MRI characteristics and the histological subtype was evaluated using Chi-Square and ANOVA tests.

Results The MRI parameters that showed a statistically significance correlation with malignant histology and thus most strongly associated with LMS were found to be: irregular contours ($p < 0.001$), intra-tumoral haemorrhagic areas ($p = 0.028$), T2-WI dark areas ($p = 0.016$), high signal intensity after contrast administration ($p = 0.005$), necrosis ($p = 0.001$), central location for unenhanced areas ($p = 0.026$), and ADC value lower than 0.88×10^{-3} mm^2/s ($p = 0.002$).

Conclusion With our work, we demonstrate the presence of seven MRI features that are statistically significant in differentiating between LMS and ALM.

Keywords Uterine leiomyosarcoma · Atypical uterine leiomyoma · Uterine tumour · Magnetic resonance imaging · Texture analysis

✉ Patrícia Freitas
patriciafreitas958@gmail.com

1 Department of Radiology, Hospital São José, Centro Hospitalar Universitário Lisboa Central, R. José António Serrano, 1150-199 Lisbon, Portugal

2 Department of Radiology, Hospital Curry Cabral, Lisbon, Portugal

3 Department of Radiology, Hospital de Santa Maria, Lisbon, Portugal

4 Department of Radiology, Instituto Portugues de Oncologia de Lisboa Francisco Gentil, Lisbon, Portugal

5 Department of Pathology, Instituto Portugues de Oncologia de Lisboa Francisco Gentil, Lisbon, Portugal

6 Nova Medical School, Lisbon, Portugal

What does this study add to the clinical work

The accurate diagnosis of LMS remains a clinical challenge.

Our study demonstrates seven MRI features that are statistically significant in differentiating between LMS and ALM: the presence of irregular contours, intra-tumoral haemorrhagic areas, T2-WI dark areas, high signal intensity after contrast administration, the presence of necrosis, central location for unenhanced areas, and an ADC value lower than 0.88×10^{-3} mm^2/s are more frequent in LMS.

🖄 Springer

Introduction

The pathologic spectrum of uterine smooth muscle tumours ranges at opposite ends between uterine leiomyomas and leiomyosarcomas.

Uterine leiomyoma is the most frequent gynaecologic neoplasm and the most common uterine tumour in women, with a prevalence reaching 70–80% among women 50 years old and older [1]. According to the World Health Organization (WHO) classification of Female Genital Tumours updated in 2020, leiomyomas can be categorized as Usual-type leiomyoma or by their different subtypes (Cellular leiomyoma; Leiomyoma with bizarre nuclei; Fumarate hydratase (FH) deficient leiomyoma; Mitotically active leiomyoma; Hydropic leiomyoma; Apoplectic leiomyoma; Lipoleiomyoma; Epithelioid leiomyoma; Myxoid leiomyoma; Cotyledonoid dissecting leiomyoma; Diffuse leiomyomatosis) (Table 1) [2, 3].

Uterine sarcoma has a mesenchymal origin and represents a rare malignant tumour (1% of all gynaecological neoplasms and 3–7% of the primary malignant tumours of the uterus) [4, 5]. Leiomyosarcoma (LMS) is derived from myometrial smooth muscle cells, typically de novo in the uterine corpus [6]. In extreme and rare cases, LMS results from sarcomatous transformation of a pre-existing leiomyoma (0.2% of cases) [6]. Among all uterine sarcomas, LMS is the most common histologic subtype (40–50% of the cases) [6]. According to WHO classification of Female Genital Tumours updated in 2020, LMS can be subcategorized as Epithelioid, Conventional (spindle cell), and Myxoid [3]. LMS is an extremely aggressive tumour with a poor prognosis, with a 5 years survival rate estimated at 17–55% [3, 6].

The literature describes some risk factors for LMS, including the black community, age at diagnosis above 60 years old, exposure to pelvic radiation, usage of tamoxifen, and retinoblastoma in childhood [4, 7].

Clinical symptoms are not a reliable indicator to differentiate leiomyoma from LMS, since both are associated with pelvic pain, abnormal bleeding, and a pelvic mass [8].

Leiomyomas are diagnosed with Magnetic Resonance Imaging (MRI) by showing low signal intensity at T2-Weighted Imaging (T2-WI) and Diffusion-Weighted Imaging (DWI) [5]. However, it may be challenging to differentiate a leiomyoma from leiomyosarcoma, specially from early-stage LMS. Up to 65% of leiomyomas manifest with degenerative changes or variant subtypes, leading to an atypical appearance on MRI [5, 9, 10].

MRI plays a crucial role in determining the diagnosis of leiomyoma and confirming its benignity. In pre-menopausal women with leiomyomas, it may be offered conservative treatments, such as myomectomy, uterine artery embolization (UAE), or hormonal therapy [5, 9]. A false diagnosis of LMS can lead to an unnecessary hysterectomy in pre-menopausal patients, but a myomectomy in cases of a posteriorly confirmed sarcoma can lead to dissemination with morcellation [5]. It is fundamental to distinguish benign leiomyomas and their variants from leiomyosarcomas, to provide the best treatment option to these patients.

Most of the studies dedicated to the differentiation between leiomyomas with atypical features and malignant uterine sarcomas, included in the same category LMS, endometrial stromal sarcoma, adenosarcoma, undifferentiated endometrial sarcoma, and other sarcomas, despite the discrepancy of its imaging features [5, 8, 11–14]. In contrast, our study intends to differentiate leiomyomas with atypical features in MRI from LMS.

Materials and methods

Patient selection

We conducted a retrospective, single-centre study, that included a total of 57 patients.

Table 1 WHO classification of Female Genital Tumours (2020)

Leiomyomas	Leiomyosarcomas
Cellular leiomyoma	Conventional (spindle cell) uterine leiomyosarcoma
Leiomyoma with bizarre nuclei	Epithelioid uterine leiomyosarcoma
Fumarate hydratase (FH) deficient leiomyoma	Myxoid uterine leiomyosarcoma
Mitotically active leiomyoma	
Hydropic leiomyoma	
Apoplectic leiomyoma	
Lipoleiomyoma	
Epithelioid leiomyoma	
Myxoid leiomyoma	
Cotyledonoid dissecting leiomyoma	
Diffuse leiomyomatosis	

Clinical data were collected from medical records and institutional databases to identify pathologically proven leiomyosarcomas and atypical leiomyomas (those presenting hyperintensity on T2-WI equal or superior to 50% compared to the myometrium).

To ensure a precise histological diagnosis, all cases were revised by a specialized pathologist, dedicated to female pelvic pathology. All cases were revised and categorized according to the new classification of the WHO classification of Female Genital Tumours updated in 2020. The study includes 31 atypical leiomyomas (ALM) and 26 LMS.

All patients performed a pelvic MRI 6 months before surgery, between January 2009 and March 2020.

The exclusion criteria include: patients whose pelvic MRI was not obtained with intravenous contrast administration or that did not cover the whole tumour; cases that were not submitted to surgical intervention; or cases without histological material available for revision. Patient selection and data are summarized in Fig. 1.

This study was approved by the institutional review board and the requirement for written informed consent was waived due to its retrospective nature.

MRI protocol

Pelvic MRI examinations were all performed in a 1.5 T MRI scanner (Intera Pulsar; Philips Medical Systems, Best, the Netherlands), with an 8-channel phased-array body coil and saturation bands. It was required a fasting period of 4–6 h prior to examination and patients were asked to empty both bowel and bladder. An anti-peristaltic agent (N-butylscopolamine bromide, 20 mg) was given to reduce bowel mobility. All patients were placed in the supine position.

In our hospital, pelvic evaluation included a fast spin-echo T2-WI acquired in three planes: axial (slice thickness, 4 mm; interslice gap, 0.4 mm), sagittal (slice thickness, 4 mm; interslice gap, 0.4 mm), and coronal (slice thickness, 4 mm; interslice gap, 0.4 mm). T1-WI was acquired in the axial plane (slice thickness, 4 mm; interslice gap, 0.4 mm). DWI with the echo-planar technique was acquired in the axial plane (slice thickness, 4 mm; interslice gap, 0.4 mm);
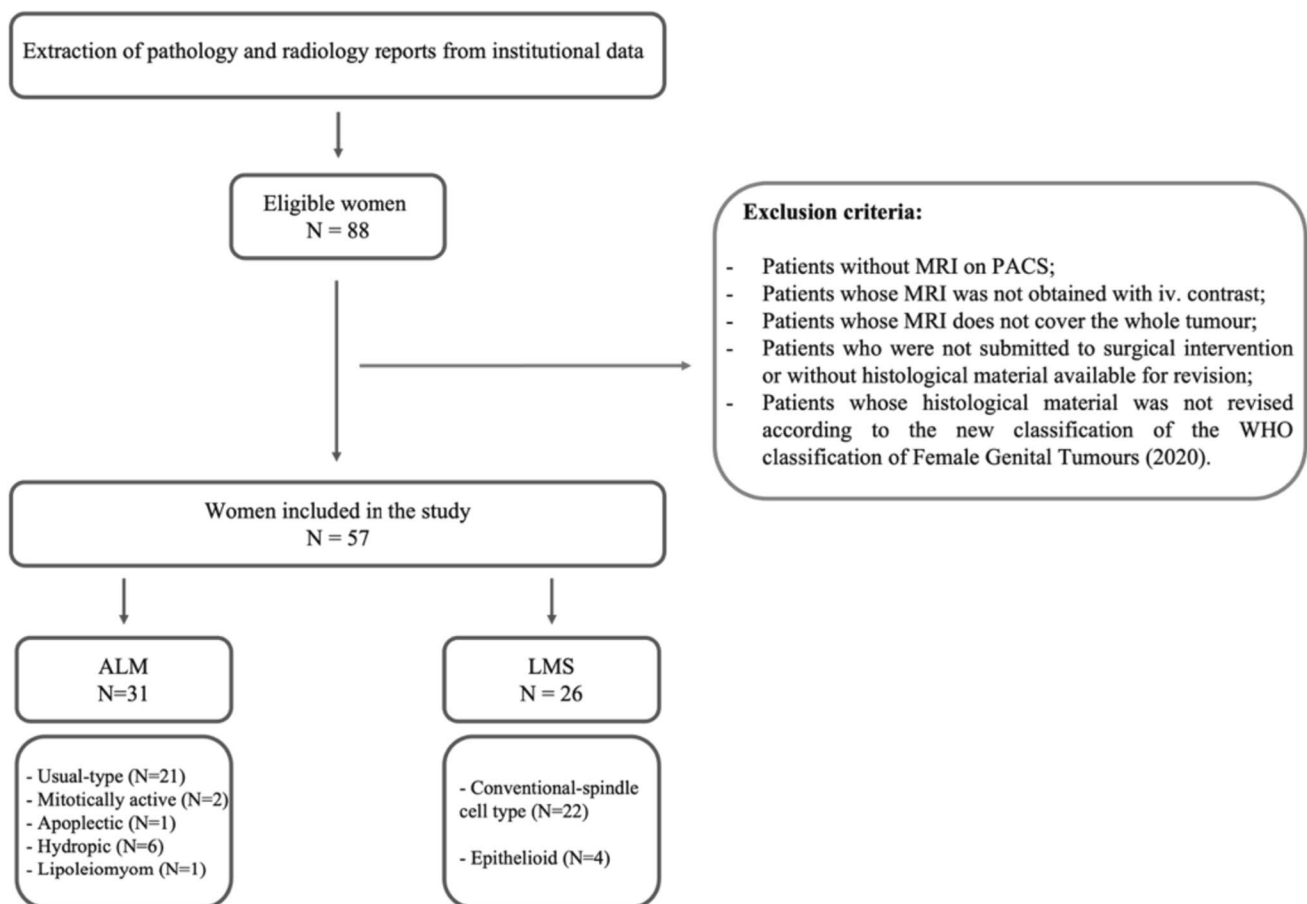

Fig. 1 Patient selection algorithm

b values of 0, 600, and 1000 s/mm^2, with the respective Apparent-Diffusion Coefficient (ADC) maps. Dynamic perfusion sequences using T1-Fat Sat (FS) (slice thickness, 3 mm; interslice gap, 0.5 mm) were acquired before and after intravenous injection of gadopentetate dimeglumine at a rate of 2 mL/s (0.1 mmol/kg of body weight—Magnevist; Bayer HealthCare AG, Leverkusen, Germany): five images were acquired after gadolinium administration (0, 25, 60, 120, and 150 s), and then a delayed post-contrast sequence (240 s) was obtained on axial plane.

MRI analysis

All exams were evaluated by a radiologist specialized in female pelvis, with more than 20 years of experience and with a European Diploma in Urogenital Radiology. The histopathological results were blinded.

In the MRI studies, the following characteristics were evaluated: age at presentation, tumour dimension and contours (irregular or smooth), presence of intra-tumoral haemorrhagic areas (areas with high signal intensity in T1-WI), T2-WI heterogeneity, T2-WI dark areas (areas of previous haemorrhage), presence of flow voids (dark spots within the vessels, which represent high flow), cystic areas (internal regular foci with a signal as bright as fluid in the bladder in T2-WI, and low signal intensity in T1-WI), and necrosis (irregular and central areas that show high signal intensity in T2-WI, but lower than the fluid in the bladder and that present lack of enhancement after contrast administration). Restriction on DWI, ADC values, signal intensity and heterogeneity after contrast administration in T1-WI sequences, and the presence and location of unenhanced areas were also evaluated.

Analysing DWI, a low signal intensity was considered when lower or equal to that of the myometrium, and a high signal intensity was defined when higher than that of the endometrium. To evaluate the ADC values of the tumours, a circular Region of Interest (ROI) was placed as large as possible within the limits of the tumour, without involving the interface or blood flow.

The presence of ascites, lymphadenopathies, and peritoneal metastases was also evaluated.

Statistical analysis

The data analysis was accomplished by using the software IBM SPSS Statistics software, version 25 (IBM Corp., Armonk, NY, USA).

Nominal or categorical variables were presented as numbers and percentages (%).

Continuous variables were expressed with means and ranges.

Continuous variables showed homogeneity of variance and descriptive analysis was performed using ANOVA. Chi-Square Tests and Fischer's exact test were used for categorical variables, to evaluate a statistically significant difference between pelvic MRI characteristics of ALM $vs.$ LMS.

Table 2 Description of the clinical data symptomatology

Clinical data	LMS ($N=26$)	ALM ($N=31$)
Asymptomatic	11	13
Lower abdominal/pelvic pain	4	5
Increased abdominal volume	1	8
Abnormal uterine bleeding	10	5

Table 3 MRI features and statistical data of ALM and LMS

MRI findings	LMS (N=26)	ALM (N=31)	p value
Dimension	116.42 ± 55.30	125.87 ± 61.37	0.547
Irregular contour	21	7	< 0.001
Intra-tumoral haemorragic areas	16	11	0.028
T2-WI dark areas	22	17	0.016
T2-WI heterogeneity	24	29	0.855
Flow voids	8	8	0.678
Cystic areas	9	15	0.294
Necrosis	15	5	0.001
ADC value	0.88 ± 0.210	1.22 ± 0.275	0.002
Central location of unenhanced areas	12	7	0.026
High signal intensity after iv. contrast	19	11	0.005
Heterogeneity after iv. contrast	23	24	0.275
Presence of unenhanced areas	20	23	0.812
Pelvic lymphadenectomy	1	0	
Peritoneal metastasis	1	0	
Free pelvic fluid	2	0	

A p value of < 0.05 was regarded as statistically significant.

Results

The population of our study was composed of 57 women, 31 diagnosed with ALM (median age of $46,03 \pm 9.354$ years old; range 30–73 years old) and 26 with LMS (median age of $56,42 \pm 11.563$ years old; range 36–86 years old).

Clinical symptoms of the symptomatic group were non-specific. Complaints included lower abdominal/pelvic pain, increased abdominal volume, and abnormal uterine bleeding (Table 2).

Out of the 31 patients diagnosed with ALM, 21 were subclassified as usual-type (67.74%), 2 mitotically active

Table 4 Distribution of the location of unenhanced areas in ALM and LMS

	Absence	Central	Random	Peripheral
ALM	57.1% (N=8)	36.8% (N=7)	50% (N=8)	100% (N=8)
LMS	42.9% (N=6)	63.2% (N=12)	50% (N=8)	0% (N=0)
Total	100% (N=14)	100% (N=19)	100% (16)	100% (N=8)

(6.45%), 1 apoplectic (3.23%), 6 hydropic (19.35%), and 1 lipoleiomyoma (3.23%). Out of the 26 patients diagnosed with LMS, 22 were subcategorized as conventional spindle cell type (84.62%) and 4 as epithelioid leiomyosarcomas (15.38%), upon histopathologic evaluation (Fig. 1).

MRI features and statistical data of ALM and LMS are summarized in Table 3.

The MRI parameters that showed a statistically significant correlation with malignant histology and thus most strongly associated with LMS were found to be:

– Irregular contours ($p < 0.001$) were documented in 28 patients, 75% ($n = 21$) corresponding to LMS and 25% ($n = 7$) to ALM;
– Intra-tumoral haemorrhagic areas ($p = 0.028$) were found in 16 patients, 68.8% ($n = 11$) corresponding to LMS and 31.3% ($n = 5$) to ALM;
– T2-WI dark areas ($p = 0.016$) were found in 39 patients, 56.4% ($n = 22$) related to LMS and 43.6% ($n = 17$) to ALM;
– High signal intensity after contrast administration ($p = 0.005$) was found in 30 patients, 63.3% ($n = 19$) corresponding to LMS and 36.7% ($n = 11$) to ALM;
– Presence of necrosis ($p = 0.001$) was found in 20 patients, 75% ($n = 15$) corresponding to LMS and 25% ($n = 5$) to ALM;

Fig. 2 MRI scans in 54-years-old postmenopausal woman, represented in sagittal T2-WI (**a**), axial b-1000 DWI (**b**), ADC map (**c**, **d**), and axial FS CE-T1-WI (**e**) sequences of the pelvis. Images show a large and heterogenous uterine tumour, with irregular contours and "T2 dark-areas" in the myometrial mass (white arrow, **a**). It is seen intra-lesional hyperintense areas in T2-WI, but still with a lower signal than the bladder, suggesting the presence of necrosis (blue arrow, **a**). This tumour shows restriction in DWI sequences and respective low signal intensity in ADC map (**c**, **d**). The mean ADC value represented in this LMS is $0.66 \pm 0.11 \times 10^{-3}$ mm^2/s, which is considered suspicious for malignancy. FS CE-T1-WI shows the presence of central unenhanced areas (orange arrow, **e**). Histology confirmed epithelioid uterine leiomyosarcoma—a malignant neoplasm with foci of necrosis (*, **f**) composed of atypical spindled to epithelioid cells with high mitotic activity (black arrow, **g**). Neoplastic cells are strongly positive for desmin (**h**)

– Central location of unenhanced areas ($p = 0.026$) was documented in 19 patients, 63.2% ($n = 12$) corresponding to LMS and 36.8% ($n = 7$) to ALM. Unenhanced areas were documented in a total of 43 patients and then categorized according to their location (Table 4). Out of the 20 leiomyosarcomas with unenhanced areas, 60% ($n = 12$) presented a central location and 40% ($n = 8$) had a random location.

– ADC value lower than $0.88 \pm 0.210 \times 10^{-3}$ mm^2/s ($p = 0.002$). The ADC value was evaluated in 26 patients. The mean and standard deviation of the ADC value in the ALM ($n = 14$) was $1.22 \pm 0.275 \times 10^{-3}$ mm^2/s and in the LMS ($n = 12$) $0.88 \pm 0.210 \times 10^{-3}$ mm^2/s.

Dimension, T2-WI heterogeneity, flow voids, cystic areas, heterogeneity after contrast administration, and the presence

of unenhanced areas did not show statistical significance (Table 3).

Discussion

This study demonstrated that the presence of irregular contours, intra-tumoral haemorrhagic areas, T2-WI dark areas, high signal intensity after contrast administration, the presence of necrosis, central location for unenhanced areas, and ADC value lower than 0.88×10^{-3} mm^2/s are statistically different between LMS and ALM, being more frequent in LMS (Figs. 2 and 3).

Our results are similar to other ones published in the literature. Lakhman et al. conducted a retrospective study of 41 women (22 ALM and 19 LMS) and verified that nodular borders, haemorrhage, presence of T2-WI dark areas, and central unenhanced areas were related to LMS; three or more
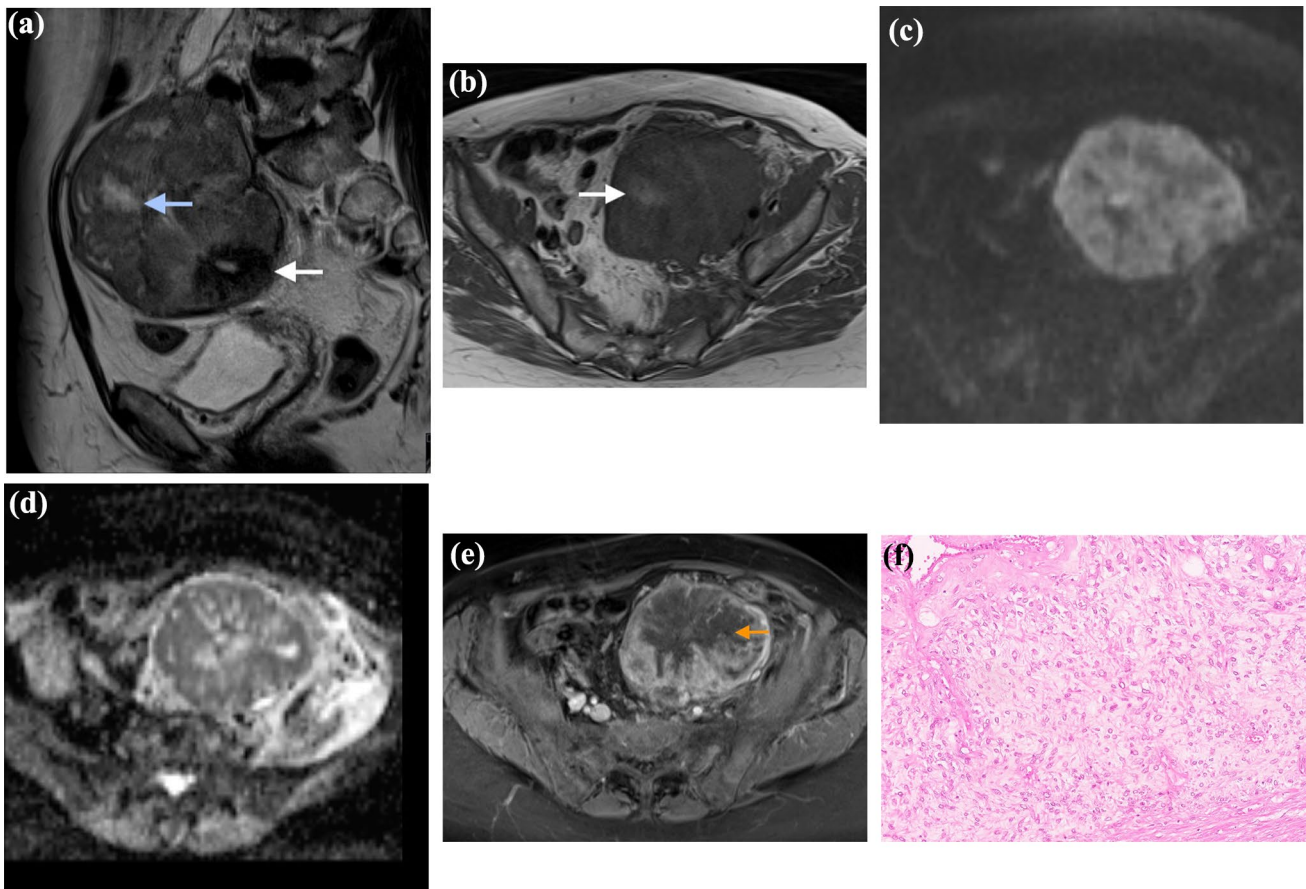
Fig. 3 MRI scans in 71-year-old postmenopausal woman, represented in sagittal T2-WI (**a**), axial T1-WI (**b**), axial b-1000 DWI (**c**), ADC map (**d**), and axial FS CE-T1-WI (**e**) sequences of the pelvis. This case illustrates a recurrence of uterine leiomyosarcoma in the left pelvic wall, in a patient submitted to a previous hysterectomy. Features that strongly associate with LMS in histopathology are present. Images show a large tumour with slightly irregular borders, "T2 dark areas" (white arrow, **a**), and necrosis (blue arrow, **a**). Also, T1-WI illustrates the presence of intralesional haemorrhage (white arrow, **b**). This tumour shows restriction in DWI sequences and respective low signal intensity in the ADC map (**c, d**). Axial FS CE-T1-WI shows the presence of central unenhanced areas (orange arrow, **e**). Histology revealed a malignant neoplasm with nested growth composed of epithelioid cells with clear cytoplasm (**f**)

Fig. 4 Sagittal T2-WI (**a**), axial T2-WI (**b**), and ADC map (**c**) sequences of the pelvis. Images depict a subserous atypical leiomyoma (white arrow, **a**), with respectively heterogeneous signal intensity on T2-WI (**a, b**). The ALM is compressed by the sacral promontory and presents growth into the abdominal cavity (**a**). The mean ADC value represented in this ALM is $1.38 \pm 0.11 \times 10^{-3}$ mm^2/s, which is not considered suspicious for malignancy according to our statistical analysis (**c**). According to the WHO classification, the histology revealed usual-type leiomyoma—intersecting fascicles of spindle eosinophilic cells with cigar-shaped nuclei and fine chromatin with small nucleoli can be observed (**d**)
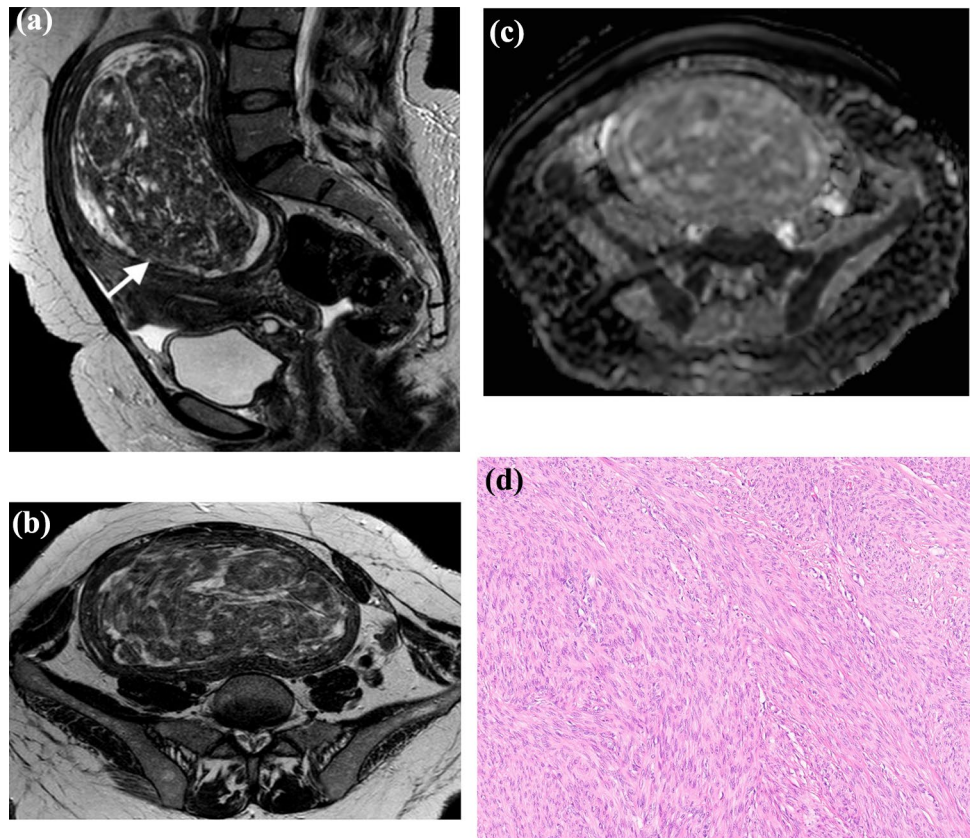
of these MRI features could accurately distinguish LMS from ALM [15]. A meta-analysis from Virarkar et al. which included eight studies with 795 patients, also concluded that high signal intensity on T1-WI and low ADC values can differentiate with accuracy LMS from leiomyomas [16].

In our study, ALM showed a mean ADC value of $1.22 \pm 0.275 \times 10^{-3}$ mm^2/s and LMS presented a mean ADC value of $0.88 \pm 0.210 \times 10^{-3}$ mm^2/s. Hence, we concluded that an ADC value equal to or lower than $0.88 \pm 0.210 \times 10^{-3}$ mm^2/s could help to differentiate LMS from ALM. Recent studies, such as Wahab et al., created a diagnostic algorithm with predictive features to diagnose malignant uterine sarcomas that validate some of our conclusions [5]. It was revealed that the presence of enlarged lymph nodes or peritoneal metastases is highly suspicious, but also that an ADC value equal to or less than 0.905×10^{-3} mm^2/s was a predictive feature for malignancy [5]. If the DWI signal of solid tissue is lower than myometrium or if it is intermediate (higher than myometrium but lower than endometrium or lymph nodes) then the tumour is most certainly benign. They also concluded that the perfusion acquisitions did not discriminate ALM from LMS, because they realised that even ALMs can be highly vascular [5].

Another study by Thomassin-Naggara et al. developed a diagnostic algorithm for preoperative MRI differentiating uterine sarcoma from leiomyoma, which included 65 patients (51 with benign lesions and 14 with malignant lesions) [17]. The authors revealed that the MRI combination of T2-WI, b-1000, and ADC features is 92.4% accurate in differentiating benign from malignant myometrial tumours [17]. Sato et al. suggested that lesions with intermediate-to-high signal intensity on DWI and low ADC value ($< 1.1 \times 10^{-3}$ mm^2/s) stratify patients at high risk of LMS [18]. Jagannathan et al. created a scoring system to identify the tumours with the highest risk of having LMS before surgery and they concluded that seven key MRI features could allow that differentiation (1. heterogeneity on T2-WI; 2. high signal intensity of the solid component on T2-WI; 3. intra-tumoral haemorrhage; 4. heterogeneous enhancement; 5. enhancing finger-like projections; 6. the presence of an ill-defined border with the myometrium on T1-WI CE; 7. central non-enhancing necrosis) [19].

Smith et al. recently published a review article denoting a mnemonic with the acronym "BET^{1}T^{2}ER check" that helps differentiate benign uterine leiomyomas from uterine sarcomas [20]. The authors concluded that the MRI imaging features that are indicative of uterine sarcoma include: irregular borders, heterogenous enhancement with central poor enhancement, T2-WI dark areas (haemosiderin and vascular signal voids), haemorrhage represented by a hyperintense signal on T1-WI, endometrial invasion and lastly restriction to diffusion [20].
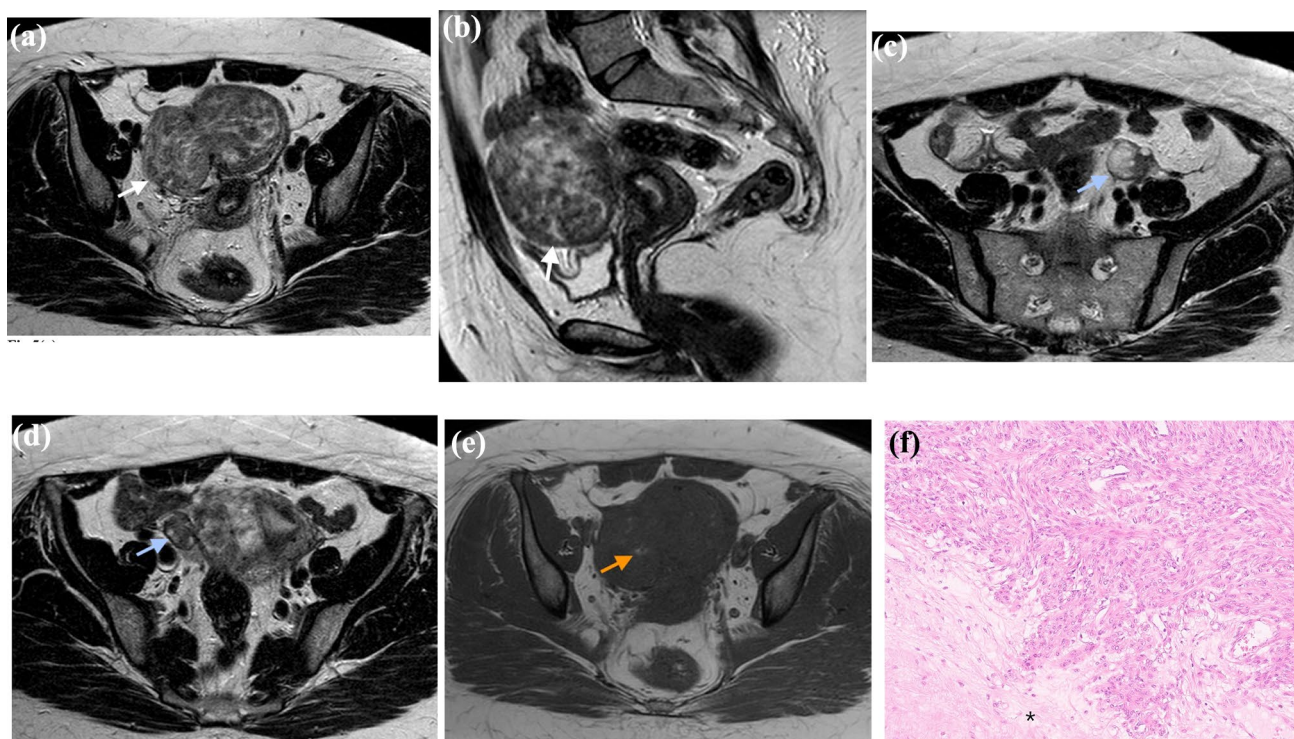
Fig. 5 Axial T2-WI (**a**, **c**, **d**), sagittal T2-WI (**b**), axial T1-WI (**e**) sequences of the pelvis. Images present atypical leiomyoma with regular contours, located in the anterior wall of the uterine body, heterogeneous, with hyperintense areas alternating with hypointense areas assuming cobblestone appearance in T2-WI (white arrows, **a–b**). This tumour assumes an hourglass appearance (**a**). Both ovaries are documented with follicular activity (blue arrows, **c–d**). On T1-WI, are depicted punctate images with high signal intensity, compatible with haemorrhagic foci (orange arrow, **e**). Even though MRI images suggest hyaline degeneration, histology revealed hydropic leiomyoma—fascicles and cords of benign smooth muscle cells transition into an area of edema (*, **f**)

Typical leiomyomas may be diagnosed with confidence at MRI, due to their classic appearance (well-demarcated and hypointense on T1-WI and T2-WI) [9]. On the other hand, LMS usually presents as a large infiltrating lesion, with ill-defined borders, irregular contours, heterogeneous intermediate-to-high signal intensity on T2-WI, and typically shows rapid growth in size [21, 22]. Sometimes it may present with necrosis and intra-lesional haemorrhagic foci [21].

Despite the significant difference in prevalence, the accurate diagnosis of LMS remains a clinical challenge. The problematic diagnosis does not refer to the leiomyomas that present with typical features in MRI, but to the ones with degenerative changes or some subtypes, which leads to an atypical appearance on MRI (Figs. 4 and 5) [5, 9]. Both entities have similar ages of presentation at diagnosis and similar clinical symptoms [15]. Also, "rapid growth" is not a distinctive feature of malignancy and may happen in both LMS and ALM [23]. Serum markers such as LDH may be elevated with LMS but also ALM, such as the cellular subtype or those with degeneration [24].

It is imperative to differentiate ALM from LMS, because treatment options vary and influence the prognosis. For a woman in post-menopause with leiomyomas, a hysterectomy can be offered [5]. However, pre-menopausal women with leiomyomas may prefer less invasive procedures, including uterine artery embolization, leiomyoma morcellation, and radiofrequency myolysis, which allows fertility preservation [5, 8, 25]. There is a concern about the risk of occult LMS found at surgery for presumed uterine leiomyomas, although it is much less frequent than previously estimated (1 leiomyosarcoma per 8300 surgeries) [26].

Our study presents some limitations. First, it is a retrospective study. Nevertheless, our radiological and histopathological reporting database has accurate recordkeeping, and every single case was revised once included in the study. Also, all the exams were read by a single radiologist, which might be considered a limitation, although the radiologist has more than 25 years of experience in urogenital radiology and is certified with the European Diploma in Urogenital Radiology (level III ESR European Training Curriculum for subspecialisation in Radiology).

Conclusion

In conclusion, this study demonstrated that the presence of irregular contours, intra-tumoral haemorrhagic areas, T2-WI dark areas, high signal intensity after contrast administration, the presence of necrosis, central location for unenhanced areas, and an ADC value lower than 0.88×10^{-3} mm^2/s are statistically different between LMS and ALM, being more frequent in LMS. This distinction is crucial to provide optimal management and appropriate surgical planning.

Declarations

References

1. Arleo EK, Schwartz PE, Hui P, McCarthy S (2015) Review of leiomyoma variants. Am J Roentgenol 205(4):912–921
2. Alran L RACS. Leiomyoma-general. PathologyOutlines.com website. https://www.pathologyoutlines.com/topic/uterusleiomyoma.html. Accessed 15 Jun 2022
3. WHO Classification of Tumours Editorial Board, editor (2020) WHO Classification of Tumours. Female Genital Tumours. 5th ed. Vol. 4. 272–285
4. Beyan E, Kanmaz AG, İnan AH, Karataşlı V, Tutar SO, Alan M, Töz E, Sancı M (2019) Evaluation of occult uterine leiomyosarcomas. Ginekol Pol 90(8):433–437
5. Abdel Wahab C, Jannot AS, Bonaffini PA, Bourillon C, Cornou C, Lefrère-Belda MA, Bats AS, Thomassin-Naggara I, Bellucci A, Reinhold C, Fournier LS (2020) Diagnostic algorithm to differentiate benign atypical leiomyomas from malignant uterine sarcomas with diffusion-weighted MRI. Radiology 297(2):361–371
6. Sousa FAE, Ferreira J, Cunha TM (2021) MR Imaging of uterine sarcomas: a comprehensive review with radiologic-pathologic correlation. Abdom Radiol 46:5687–5706
7. Lucas R, Cunha TM (2019) Uterine sarcomas. Medical radiology. Springer Verlag, pp 209–224
8. Stewart EA, Barbieri RL, Goff B, Falcone T, Levine D. Uterine fibroids (leiomyomas): differentiating fibroids from uterine sarcomas Section Editors
9. Rio G, Lima M, Gil R, Horta M, Cunha TM (2019) T2 hyperintense myometrial tumors: can MRI features differentiate leiomyomas from leiomyosarcomas? Abdom Radiol 44(10):3388–3397
10. Kubik-Huch RA, Weston M, Nougaret S, Leonhardt H, Thomassin-Naggara I, Horta M, Cunha TM, Maciel A, Rockall A, Forstner R (2018) European Society of Urogenital Radiology (ESUR) guidelines: MR imaging of leiomyomas. Eur Radiol 28(8):3125–3137
11. Nakagawa M, Nakaura T, Namimoto T, Iyama Y, Kidoh M, Hirata K, Nagayama Y, Yuki H, Oda S, Utsunomiya D, Yamashita Y (2019) Machine learning to differentiate T2-weighted hyperintense uterine leiomyomas from uterine sarcomas by utilizing multiparametric magnetic resonance quantitative imaging features. Acad Radiol 26(10):1390–1399
12. Suzuki A, Aoki M, Miyagawa C, Murakami K, Takaya H, Kotani Y, Nakai H, Matsumura N (2019) Differential diagnosis of uterine leiomyoma and uterine sarcoma using magnetic resonance images: a literature review. Healthcare 7(4):158
13. Himoto Y, Kido A, Sakata A, Moribata Y, Kurata Y, Suzuki A, Matsumura N, Shitano F, Kawahara S, Kubo S, Umeoka S, Minamiguchi S, Mandai M (2021) Differentiation of uterine low-grade endometrial stromal sarcoma from rare leiomyoma variants by magnetic resonance imaging. Sci Rep. https://doi.org/10.1038/s41598-021-98473-z
14. Libertini M, Hallin M, Thway K, Noujaim J, Benson C, van der Graaf W, Jones RL (2021) Gynecological sarcomas: molecular characteristics, behavior, and histology-driven therapy. Int J Surg Pathol 29:4–20
15. Lakhman Y, Veeraraghavan H, Chaim J, Feier D, Goldman DA, Moskowitz CS, Nougaret S, Sosa RE, Vargas HA, Soslow RA, Abu-Rustum NR, Hricak H, Sala E (2017) Differentiation of uterine leiomyosarcoma from atypical leiomyoma: diagnostic accuracy of qualitative MR imaging features and feasibility of texture analysis. Eur Radiol 27(7):2903–2915
16. Virarkar M, Diab R, Palmquist S, Bassett R, Bhosale P (2020) Diagnostic Performance of MRI to differentiate uterine leiomyosarcoma from benign leiomyoma: a meta-analysis. J Belg Soc Radiol. https://doi.org/10.5334/jbsr.2275
17. Thomassin-Naggara I, Dechoux S, Bonneau C, Morel A, Rouzier R, Carette MF, Daraï E, Bazot M (2013) How to differentiate benign from malignant myometrial tumours using MR imaging. Eur Radiol 23(8):2306–2314
18. Sato K, Yuasa N, Fujita M, Fukushima Y (2014) Clinical application of diffusion-weighted imaging for preoperative differentiation between uterine leiomyoma and leiomyosarcoma. Am J Obstet Gynecol 210(4):368.e1-368.e8
19. Jagannathan JP, Steiner A, Bay C, Eisenhauer E, Muto MG, George S, Fennessy FM (2021) Differentiating leiomyosarcoma from leiomyoma: in support of an MR imaging predictive scoring system. Abdom Radiol 46(10):4927–4935
20. Smith J, Zawaideh JP, Sahin H, Freeman S, Bolton H, Addley HC (2021) Differentiating uterine sarcoma from leiomyoma: BET[1]T[2] ER Check! Br J Radiol 94(1125):20201332
21. Santos P, Cunha TM (2015) Uterine sarcomas: clinical presentation and MRI features. Diagn Interv Radiol 21(1):4–9
22. Hindman N, Kang S, Fournier L, Lakhman Y, Nougaret S, Reinhold C, Sadowski E, Huang JQ, Ascher S (2022) MRI evaluation

of uterine masses for risk of leiomyosarcoma: a consensus statement. Radiology. https://doi.org/10.1148/radiol.211658

23. Brölmann H, Tanos V, Grimbizis G, Ind T, Philips K, van den Bosch T, Sawalhe S, van den Haak L, Jansen FW, Pijnenborg J, Taran FA, Brucker S, Wattiez A, Campo R, O'Donovan P, de Wilde RL (2015) Options on fibroid morcellation: a literature review. Gynecol Surg 12(1):3–15

24. Matsuda M, Ichimura T, Kasai M, Murakami M, Kawamura N, Hayashi T, Sumi T (2014) Preoperative diagnosis of usual leiomyoma, atypical leiomyoma, and leiomyosarcoma. Sarcoma 2014:1–6

25. Pron G (2015) Magnetic resonance-guided high-intensity focused ultrasound (MRgHIFU) treatment of symptomatic uterine fibroids: an evidence-based analysis. Ont Health Technol Assess Ser 15(4):1–86

26. Pritts EA, Vanness DJ, Berek JS, Parker W, Feinberg R, Feinberg J, Olive DL (2015) The prevalence of occult leiomyosarcoma at surgery for presumed uterine fibroids: a meta-analysis. Gynecol Surg 12(3):165–177